Dynamic Order-to-Metastable-Disorder Vortex Matter Transition in $Bi_2Sr_2CaCu_2O_{8+\delta}$

B. Kalisky,[1,2,*] Y. Myasoedov,[2] A. Shaulov,[1] T. Tamegai,[3] E. Zeldov,[2] and Y. Yeshurun[1]

[1]*Institute for Superconductivity, Department of Physics, Bar-Ilan University, Ramat-Gan, Israel*
[2]*Department of Condensed Matter Physics, Weizmann Institute, 76100 Rehovot, Israel*
[3]*Department of Applied Physics, The University of Tokyo, Hongo, Bunkyo-ku, Tokyo 113-8656, Japan*

(Received 13 June 2006; published 6 March 2007)

Magneto-optical measurements of transient vortex states in $Bi_2Sr_2CaCu_2O_{8+\delta}$ show enhanced effects of metastability in prism-shaped as compared to platelet crystals including a significant shift of the second magnetization peak and qualitatively different dynamics. In contrast to platelets, where dislocations are generated only at the sample edges, we propose that in prism samples the dislocations are generated dynamically in the entire sample due to distributed surface barriers. As a result, a dynamic phase transition from a Bragg glass to a metastable disordered phase may occur well below the thermodynamic transition field.

DOI: 10.1103/PhysRevLett.98.107001 PACS numbers: 74.25.Qt, 64.60.Cn, 74.25.Dw, 74.72.Hs

It is widely accepted that vortex matter in the presence of weak point disorder forms a quasiordered or a Bragg glass phase (BrG) in the low-temperature–low-field region of the B-T phase diagram [1]. This phase is characterized by the absence of dislocations and by weak pinning. As the field is increased, the BrG undergoes a disorder-driven first-order transition into a disordered phase (DP), which is characterized by a high density of dislocations (comparable to the density of vortices) in the equilibrium ground state [2]. This DP is strongly pinned, giving rise to the second magnetization peak (SMP) in high-temperature superconductors [3] or the peak effect (PE) in low-T_c materials at the order-disorder (OD) transition [4]. In this Letter, we wish to understand what happens when a high density of nonequilibrium dislocations is created in the region of the B-T phase diagram where the BrG phase is the equilibrium state. Such nonequilibrium dislocations can be created either statically or dynamically. The ''static'' route is readily achievable by field cooling through the PE or by field-down ramping through the SMP, giving rise to a metastable DP that is highly pinned and that can be described as a supercooled state of the high-field thermodynamic DP [4–7]. The ''dynamic'' route, however, is much more intriguing and challenging both experimentally and theoretically. When the vortex lattice is depinned by a driving force in the presence of point disorder, dislocations are created dynamically due to plastic deformations at the initial stages of lattice motion [8]. However, the concentration of such dynamically formed dislocations apparently always remains low, and, hence, the state of the lattice remains close to the original BrG phase and no metastable DP is formed. In order to create a high concentration of dislocations, a much stronger perturbation is therefore required. Such a strong perturbation so far was achieved experimentally only by forcing the vortices to penetrate through the rough edges of the sample either by field ramp-up or by transport current [6,7,9,10]. In this case, a high concentration of dislocations is generated at the sample edges forming the metastable DP, whereas the bulk of the sample acts as a drain region where the dislocations are annealed either thermally or dynamically [7,9–11].

In this Letter, we demonstrate how a high concentration of out-of-equilibrium dislocations can be generated dynamically throughout the entire sample using distributed surface disorder. When the dislocations are generated at the sample edges only, the resultant metastable DP is relatively short-lived due to the small ''edge-to-volume'' ratio. As a result, the metastable phase can be observed only in a relatively narrow region of ''field–temperature–time'' phase space below the thermodynamic OD transition. In contrast, we show here that in the case of a distributed formation of dislocations a unique regeneration mechanism continuously revives the metastable disorder, thus producing a robust metastable phase that is dynamically stable over an extended region of the phase diagram. As a result, the metastability effects become dominant and result in a significant shift of the apparent OD transition.

Three pairs of $Bi_2Sr_2CaCu_2O_{8+\delta}$ platelet and prism samples were prepared, each pair cut from a larger parent crystal. We present here the results of one of the pairs ($T_c = 92$ K); the others show the same qualitative behavior. The crystal was first cut into two $2.5 \times 1.4 \times 0.1$ mm^3 platelets. One of these was polished into a long prism with a $\sim 10°$ angle between the tilted facets and the base ($\parallel ab$ plane). In prism geometry, the surface barriers (SB) are distributed over the entire surface of the tilted facets [12], and, hence, metastable phenomena can be substantially affected. The induction distribution across the ab surface of the platelet and prism samples was imaged magneto-optically, while the external field H was stepwise changed or swept at a constant rate dH/dt (4–1600 Oe/s). Enhanced metastability phenomena were observed in the temperature range 25–39 K, where SB, rather than geometrical barriers, are the dominant source of irreversibility [13]. Snapshots of the induction distribution were taken successively, using iron-garnet indicators with in-plane anisotropy and a CCD camera.

Figure 1(a) shows the induction profiles measured in the platelet sample while the field was increased from 0 to 850 Oe in 140 s after zero-field cooling to 31 K. The profiles exhibit a double-dome shape at low fields in the BrG phase, reflecting the combined effects of geometrical barriers and low bulk pinning [14]. At elevated fields, above the thermodynamic OD transition $B_{od} \sim 400$ G, Bean profiles are obtained indicating strong bulk pinning in the DP. At intermediate fields, a sharp change in slope (''break'') is observed, indicating a point on the flux front B_f separating between the low-current-density BrG phase and the high-current-density disordered state [5,7,10]. Note, however, that on field ramp-up this break [black points in Fig. 1(a)] occurs at $B_f < B_{od}$ due to the injection of the metastable DP through the SB at the sample edges as reported previously [7]. As the front propagates towards the sample interior, the induction at the front B_f increases.

The prism sample shows significantly different profiles [Fig. 1(b)]. As geometrical barriers are absent in this geometry [12–14], the profiles have a Bean-like shape at low fields even in the absence of bulk pinning due to the equilibrium magnetization profile and the distributed SB along the tilted facets [12]. As in the platelet, the DP at high fields is observable by the increased slope of the profiles due to enhanced bulk pinning. Note that the formation of the metastable DP, as indicated by a break in the profiles, appears at significantly lower B in the prism (~200–315 G) as compared to the platelet (~275–315 G), indicating the survival of a metastable phase much further below B_{od}.

The enhanced robustness of the metastable DP in the prism is also demonstrated in ''local magnetization loops'' $dB/dx \sim j$ vs B shown in Fig. 2 for $x = -630$ μm. The arrival of the high-j metastable DP at x on the ascending field is manifested by a sudden increase in the local $|dB/dx|$, giving rise to the SMP. The data for the ascending branches clearly show that the SMP in the prism substantially precedes that of the platelet, indicating the enhanced stability of the metastable DP in the prism. Note, however, that on the descending branch the SMP appears at the *same* B in both samples [15]. Similar results were obtained for all measured temperatures (25–39 K) and dH/dt (4–1600 Oe/s).

Figure 3(a) shows the SMP field B_{SMP} on ascending and descending field ramps of 32 Oe/s in the two samples at various T. Here we define B_{SMP} as the midpoint between the onset and the peak locations of the SMP; other definitions [7] lead to similar conclusions. Remarkably, the prism and platelet show an almost identical $B_{SMP}(T)$ line on the descending branch. On the ascending branch, however, there are significant differences: While for the platelet sample the ascending $B_{SMP}(T)$ is very similar to the descending line, the ascending prism $B_{SMP}(T)$ resides at significantly lower fields. Note that the $B_{SMP}(T)$ lines have a positive slope due to inverse melting behavior [16] and the enhanced lifetime of the metastable DP at lower T [7]. Figures 3(b) and 3(c) show B_{SMP} at 29 and 31 K, respectively, in the two samples for various dH/dt. Again, the line measured on the ascending branch is substantially lower in the prism, while the rest of the lines are nearly the same. Moreover, B_{SMP} shows a large shift to lower B upon increasing dH/dt.

A deeper understanding of the metastability mechanism can be gained from examining the dynamics of the metastable DP front propagation. Figure 4 shows the location of the front x_f relative to the sample edge d as a function of time at $T = 29$ K and sweep rate of 4 Oe/s. Remarkably, while the front in the prism propagates at a constant velocity dx_f/dt from the moment of its inception at the

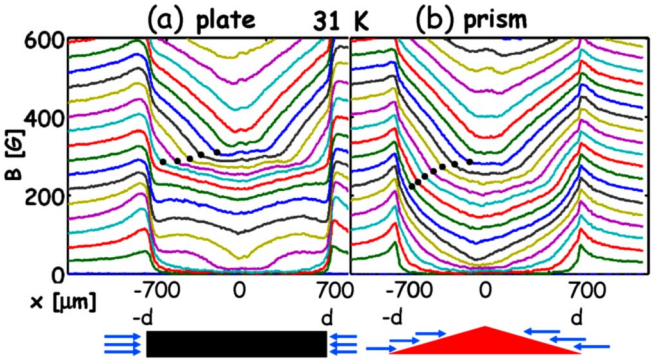

FIG. 1 (color online). Induction profiles $B(x)$ measured in (a) the platelet and (b) the prism while increasing the field from 0 to 850 Oe in 140 s after zero-field cooling to 31 K. The circles mark a typical break in the profile. The bottom of each panel illustrates cross sections of the samples. Arrows illustrate the injection of disordered vortices into the sample.

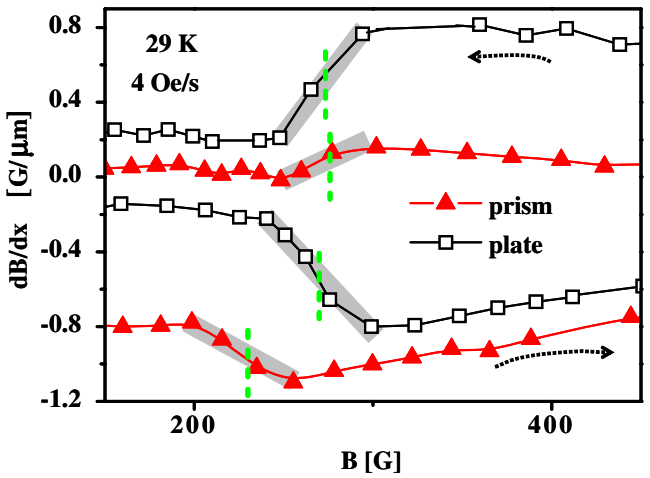

FIG. 2 (color online). Local magnetization loops, $j \sim dB/dx$ vs B, taken at $x = -630$ μm ($x_f = 70$ mm), with a sweep rate of 4 Oe/s at 29 K, for the prism and platelet samples. The transition region between the onset and the peak is shadowed, and the middle of this region—dotted line—is adopted as the transition field.

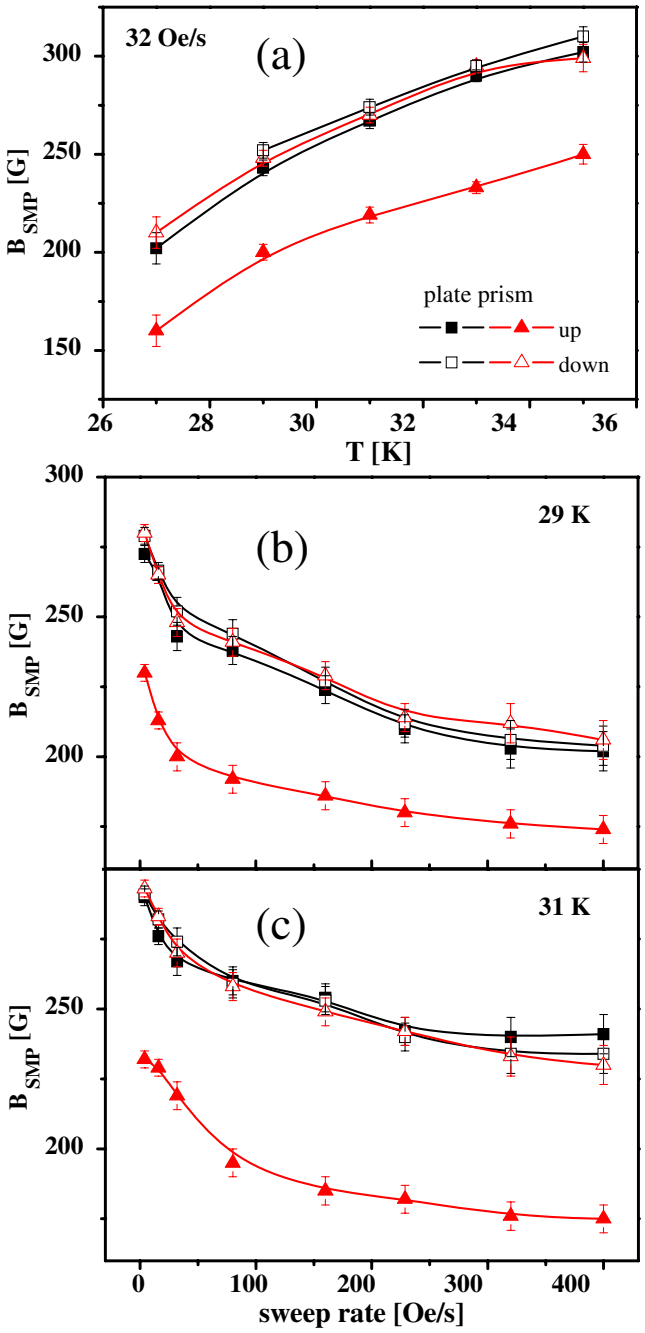

FIG. 3 (color online). The SMP for the prism (triangles) and platelet (squares) samples on ascending (solid) and descending (empty) field ramps (a) vs T for 32 Oe/s and vs dH/dt for (b) 29 and (c) 31 K.

edge (the straight line through the data), the front in the platelet accelerates gradually from zero to a final constant velocity. We can understand this marked difference as follows.

In a platelet, the front propagation is determined by competition between the injection rate of the metastable DP through the edges and the annealing rate in the bulk, which is determined by the lifetime of the metastable phase $\tau(B, T)$. Let us first consider a simplified situation in which H is ramped up suddenly to a value such that the entire sample is in the metastable DP, resulting in a Bean profile with a high slope j_h characterizing the DP. At time t after the ramp, the central part of the sample, where B is such that $\tau(B) \leq t$, will be annealed into the BrG phase characterized by the Bean profile with a lower j_l (see Fig. 4, inset). With increasing time, the annealing process will result in an outward front propagation described by the condition that at B_f the lifetime $\tau(B_f) = t$ and, hence, $dB_f/dt = 1/(\partial\tau/\partial B)|_{B=B_f}$ [7]. Since the location of the front is $x_f = (H - B_f)/j_h$ (neglecting relaxation), this argument can be readily extended to the case of a sweeping field dH/dt:

$$v_f = \frac{\partial x_f}{\partial t} = \frac{1}{j_h}\frac{dH}{dt} - \frac{1}{j_h}\frac{1}{(\partial\tau/\partial B)_{B=B_f}}. \quad (1)$$

The first term on the right-hand side of Eq. (1) describes the injection rate of the metastable DP, and, thus, in the absence of annealing the front propagates at its maximum velocity $v_f^* = (1/j_h)dH/dt$. The second term describes the annealing rate, which impedes the propagation of the metastable DP into the sample. At fields B significantly below B_{od}, the lifetime $\tau(B)$ as well as $d\tau/dB$ are very small; hence, the annealing rate is high, and the metastable DP cannot be sustained in the bulk resulting in $x_f = 0$. When B at the sample edges reaches a certain value at which the injection rate equals the annealing rate, v_f starts to grow gradually from zero. This gradual acceleration is clearly seen in the platelet data in Fig. 4 as emphasized by the solid curve. As B increases towards B_{od}, the lifetime $\tau(B)$ as well as $d\tau/dB$ increase rapidly diverging at the thermodynamic B_{od} [7]. As a result, the annealing rate

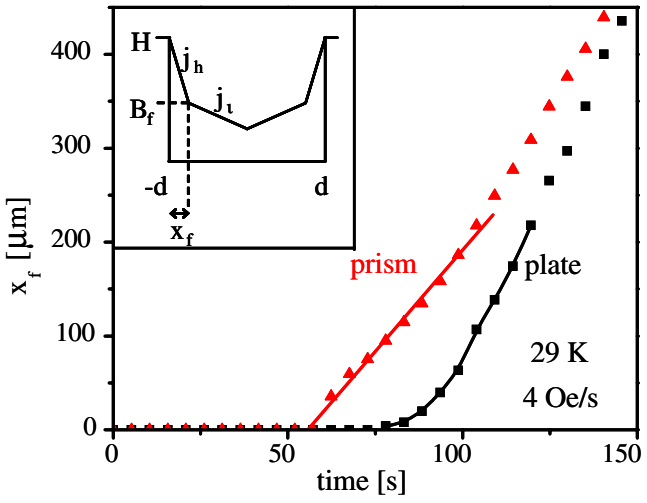

FIG. 4 (color online). The location of the front x_f as a function of time at $T = 29$ K and field sweep up at 4 Oe/s, for the plate (squares) and prism (triangles) samples.

vanishes, and v_f approaches its saturation value $v_f^* = (1/j_h)dH/dt$ determined solely by the injection rate. Indeed, the linear growth rate of x_f at higher fields in Fig. 4 equals v_f^* calculated from dH/dt and the measured j_h from the field profiles. This asymptotic behavior has been confirmed for all sweep rates and temperatures.

In contrast to the platelet, in the prism sample v_f is essentially constant from the moment of its nucleation and is approximately equal to the saturation velocity v_f^*. According to Eq. (1), it implies that the annealing process in the prism does not play a role in determining the front dynamics. This surprising result can be understood as follows. On the atomic level, the tilted facets of the prism can be thought of as a staircase with the height of each step corresponding to one or several CuO_2 layers due to some surface roughness. As a result, while moving deeper into the prism upon increasing the field, the line vortices have to elongate through local penetration of new pancakes at each step. Each addition of a pancake, or a stack of several pancakes, involves activation over local position-dependent SB [12,13]. These random SB distributed over the facets introduce local lattice distortions and inject ''fresh'' dislocations as the lattice moves into the sample. At low fields for which the balance between the injection and annealing rates in Eq. (1) is negative, no metastable DP can be nucleated, since the lifetime of dislocations is too short. However, when B reaches a critical value $B_{\mathrm{dod}} < B_{\mathrm{od}}$ for which this balance becomes positive, a local nucleation of a metastable region at the edge of the sample occurs. We argue that B_{dod} is the dynamic OD transition field, which depends on vortex velocity, above which the metastable DP becomes dynamically stable. From this moment, the annealing can no longer impede the front propagation, and, hence, v_f will be determined only by the sweep rate $(1/j_h)dH/dt$. This is due to the fact that, as the DP is forced to ''climb up'' the disordered staircase, there is a sufficient continuous supply of fresh dislocations in order to overcome the annihilation process of dislocations. We note that high resolution vortex imaging is required to obtain direct information regarding the actual amount of dynamic topological disorder [17].

The above observations may have a much broader meaning. In a regular platelet sample, the dislocations are generated only at the sample edges; therefore, in transport measurements at constant field, for example, the metastable DP will penetrate only up to a distance given by the product of the lattice velocity and the lifetime $\tau(B)$. Since for any $B < B_{\mathrm{od}}$, $\tau(B)$ is finite, the metastable DP occupies only a limited region near the sample edge and, therefore, is unstable in both the thermodynamic and the dynamic sense. On the other hand, in the presence of surface roughness such as in the prism, or, more generally, for any form of a low concentration of strong pinning centers, dislocations are generated dynamically also in the bulk of the sample. In this case, a new transition field $B_{\mathrm{dod}} < B_{\mathrm{od}}$ exists, above which the generation rate of dislocations exceeds the annealing rate, and as a result the metastable DP becomes dynamically stable and will occupy the entire sample. Since the generation and annealing rates are velocity-dependent, this mechanism will give rise to a new velocity-driven dynamic phase transition from an ordered lattice to a metastable disordered phase.

This project was supported by the German–Israel Foundation (GIF), Israel Science Foundation (ISF)—Center of Excellence Program (Grant No. 828/05)—and the Heinrich Hertz Minerva Center for High Temperature Superconductivity.

*Electronic address: beena.kalisky@weizmann.ac.il

[1] T. Giamarchi and P. LeDoussal, Phys. Rev. B **55**, 6577 (1997); D. R. Nelson, Phys. Rev. Lett. **60**, 1973 (1988); *High Magnetic Fields: Applications in Condensed Matter Physics, Spectroscopy*, edited by T. Giamarchi and S. Bhattacharya (Springer, New York, 2002), p. 314.
[2] J. Kierfeld and V. Vinokur, Phys. Rev. B **61**, R14 928 (2000).
[3] M. Daeumling, J. M. Seuntjens, and D. C. Larbalestier, Nature (London) **346**, 332 (1990); T. Nishizaki, T. Naito, and N. Kobayashi, Phys. Rev. B **58**, 11 169 (1998).
[4] S. Bhattacharya and M. J. Higgins, Phys. Rev. Lett. **70**, 2617 (1993); Phys. Rev. B **52**, 64 (1995); R. Wordenweber, P. H. Kes, and C. C. Tsuei, Phys. Rev. B **33**, 3172 (1986).
[5] C. J. van der Beek *et al.*, Phys. Rev. Lett. **84**, 4196 (2000).
[6] W. Henderson *et al.*, Phys. Rev. Lett. **77**, 2077 (1996).
[7] B. Kalisky *et al.*, Phys. Rev. B **68**, 224515 (2003); **67**, 140508(R) (2003); B. Kalisky, A. Shaulov, and Y. Yeshurun, Phys. Rev. B **68**, 012502 (2003).
[8] C. J. Olson, C. Reichhardt, and F. Nori, Phys. Rev. Lett. **81**, 3757 (1998); M. C. Marchetti, A. A. Middleton, and T. Prellberg, Phys. Rev. Lett. **85**, 1104 (2000).
[9] M. Marchevsky, M. J. Higgins, and S. Bhattacharya, Nature (London) **409**, 591 (2001); S. N. Gordeev *et al.*, Nature (London) **385**, 324 (1997); Y. Paltiel *et al.*, Nature (London) **403**, 398 (2000); H. Kupfer *et al.*, Phys. Rev. B **63**, 214521 (2001).
[10] D. Giller *et al.*, Phys. Rev. Lett. **84**, 3698 (2000).
[11] Y. Paltiel *et al.*, Phys. Rev. Lett. **85**, 3712 (2000).
[12] N. Morozov *et al.*, Physica (Amsterdam) **291C**, 113 (1997).
[13] D. Majer, E. Zeldov, and M. Konczykowski, Phys. Rev. Lett. **75**, 1166 (1995); R. A. Doyle *et al.*, Physica (Amsterdam) **308C**, 123 (1998).
[14] E. Zeldov *et al.*, Phys. Rev. Lett. **73**, 1428 (1994).
[15] Note that in the platelet sample (Fig. 2) the SMP appears at essentially the same B on ascending and descending branches when plotted vs local induction B. The SMP appears at a higher B on an ascending branch when plotted vs H due to the difference between B and H. See Khaykovich *et al.*, Phys. Rev. Lett. **76**, 2555 (1996).
[16] N. Avraham *et al.*, Nature (London) **411**, 451 (2001).
[17] Y. Fasano *et al.*, Phys. Rev. B **66**, 020512(R) (2002).